

## Core polarization and neutron halos

F Barranco<sup>1</sup>, R A Broglia<sup>2,3,4</sup>, A Idini<sup>5</sup>, G Potel<sup>6,7,8</sup>, E Vigezzi<sup>3</sup>

<sup>1</sup> Departamento de Física Aplicada III, Escuela Superior de Ingenieros, Universidad de Sevilla, 41092 Sevilla, Spain

<sup>2</sup> Dipartimento di Fisica, Università degli Studi di Milano, 20123 Milano, Italy

<sup>3</sup> INFN Sezione di Milano, 20123 Milano Italy

<sup>4</sup> The Niels Bohr Institute, University of Copenhagen, Denmark

<sup>5</sup> Institut für Kernphysik, Technische Universität Darmstadt, 64289 Darmstadt, Germany

<sup>6</sup> Lawrence Livermore National Laboratory, Livermore, CA 94551, USA

<sup>7</sup> National Superconducting Cyclotron Laboratory, Michigan State University, East Lansing, MI 48824, USA

<sup>8</sup> Department of Physics and Astronomy, Michigan State University, East Lansing, MI 48824-1321, USA

E-mail: vigezzi@mi.infn.it

**Abstract.** The effects of core polarization on the structure of Li and Be halos and their consequences on one- and two-neutron transfer reactions are discussed.

### 1. Introduction

There exists experimental evidence pointing to the fact that core polarization plays an important role in the structure of the one- and two-neutron halo nuclei  $^{11}\text{Li}$  and  $^{11}\text{Be}$ ,  $^{12}\text{Be}$ , as well as of the unbound nucleus  $^{10}\text{Li}$ . Particularly relevant in this regard are the parity inversion of the ground state of  $^{10}\text{Li}$  and  $^{11}\text{Be}$  with respect to mean field predictions, and the cross sections associated with knockout reactions and with one- and two-neutron transfer reactions leading to excited states of the  $^{10}\text{Be}$  and  $^9\text{Li}$  cores, like  $^{11}\text{Be}(p,d)^{10}\text{Be}$  or  $^{11}\text{Li}(p,t)^9\text{Li}$  (see [1] for a recent review). While the interweaving of single-particle motion and zero-point fluctuations renormalizes the ground state mean field properties in all nuclei, its effects are particularly relevant in the weakly bound, easily polarizable halo nuclei [2]. This paper summarizes results obtained [3, 4, 5, 6] by treating explicitly the basic processes involving the collective vibrations of the core, which are associated with the diagrams shown in figure 1. The polarization diagram (figure 1(a)) describes the emission and reabsorption of a phonon by a valence neutron which then increases its binding energy. The correlation diagram (figure 1(b)) accounts for the Pauli blocking of ground state correlations: due to the particle-vibration coupling, there are processes contributing to the ground state energy of the core, in which a neutron, initially in a hole state below the Fermi energy, virtually emits a phonon and jumps into an unoccupied state above the Fermi energy, finally returning to its initial state by reabsorbing the phonon. These processes become partially forbidden when a valence neutron is added in the same state to form the halo. This loss of correlation energy associated with core fluctuations must be subtracted in calculating the binding energy of the valence neutron. This effect depends in a specific way on the angular momentum and parity of the single-particle states and of the phonons. We note



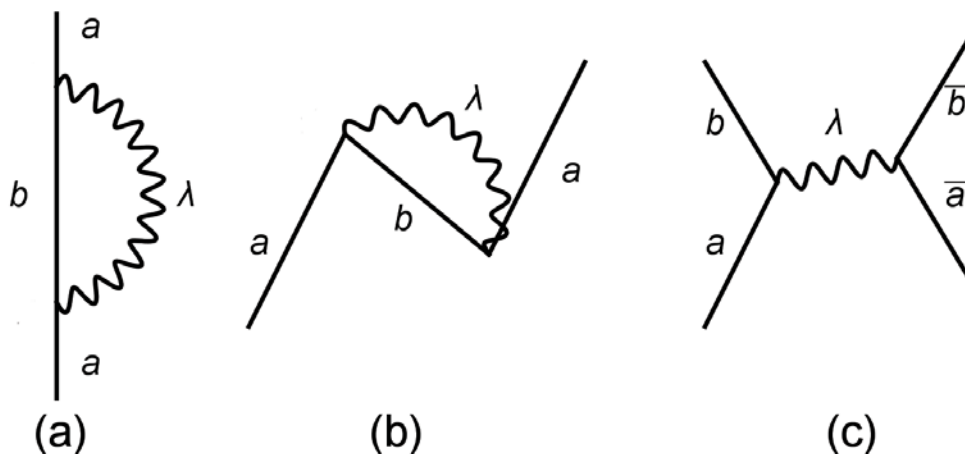


**Figure 1.** Processes coupling quasiparticles with collective vibrations, which renormalize the normal and abnormal densities obtained in mean field calculations: (a) polarization, (b) correlation, (c) induced pairing interaction, processes.

that a similar effect is operative in the pairing channel, associated with the blocking of collective pairing fluctuations. The latter effect, which tends to act equally on all the valence orbitals, will not be taken into account in the following. Finally, diagram (c) represents the exchange of collective vibrations between pairs of neutrons, which must be added to the bare N-N interaction and represents an essential contribution to the binding of two-neutron halos.

The importance of diagram (a) (associated with quadrupole vibrations, see below) for the phenomenon of parity inversion in halo nuclei has been recognized since a long time [7, 8]. Its effects on the structure of  $^{11}\text{Be}$  and  $^{12}\text{Be}$  have been studied treating the core as a deformed rotor [9, 10, 11]. It is well known that the couplings with core lead to important modifications of the radial form factors entering DWBA calculations for transfer reactions [12, 13]. They have been considered in the calculation of one-neutron transfer reactions involving  $^{11}\text{Be}$ , both within DWBA [10, 14], and, more recently, within the Faddeev scheme [15], as well as in the calculation of breakup [16]. However these calculations assume that the hole states are completely filled, and diagram (b) has not been considered. The effect of Pauli principle associated with pairing fluctuations was instead included in the calculations of Myo *et al.* (see [17] and [18] and references therein), who, on the other hand, have not included the coupling to quadrupole surface vibrations. An early recognition of the importance of diagram (c) for the binding for two-neutron halos can be found in [19].

We notice that the dynamical processes depicted in figure 1 are taken into account to some extent in calculations of the halo structure which do not include the internal core degrees of freedom, but use parity-dependent neutron-core potentials to fit the observed position of single-particle levels in one-neutron halos, and density-dependent interactions to reproduce the experimental binding energies in two-neutron halos (see for example [20, 21, 22]). Within such an approach, however, it is not straightforward to recognize the common origin of a variety of effects observed in one- and in two-neutron halos. We also remark that reproducing the structure of halo nuclei still represents a challenge for ab initio calculations [23, 24, 25].

## 2. Theory and results

The one-neutron halo system will be described by the Hamiltonian [26]

$$\hat{H} = \hat{H}_F + \hat{H}_B + \delta\hat{U}, \quad (1)$$

where  $\hat{H}_F$  is associated with the mean field,  $H_B$  is associated with the dynamics of the core and  $\delta\hat{U}$  couples single-particle motion with the collective vibrations. We assume that the mean field potential is a spherical Saxon-Woods potential  $U(r)$  parametrized as in [27] (equations (2-181, 2-182)), except for a slight adjustment of the depth. We include states of angular momentum quantum numbers  $s_{1/2}, p_{1/2}$  and  $d_{5/2}$ , obtained by solving the Schrödinger equation taking into account the (discretized) continuum, within a box of radius  $R$  up to an energy  $E_{cut}$ .

We include collective vibrations of multipolarity  $\lambda^\pi = 1^-, 2^+$  and  $3^-$ . They are calculated within QRPA using a separable force, with a coupling constant adjusted to reproduce the energy and the transition probability of the lowest states. The coupling term is given by

$$\delta\hat{U} = \sum_{\lambda\mu} \frac{\beta_\lambda}{\sqrt{2\lambda+1}} (i)^{-\lambda} \left\{ \left[ \hat{\Gamma}_{\lambda\mu}^\dagger + (-)^{\lambda+\mu} \hat{\Gamma}_{\lambda-\mu} \right] \times \sum_{kk'} \langle k | -R_0 \frac{dU}{dr} Y_{\lambda\mu}^* | k' \rangle a_k^\dagger a_{k'} \right\} \quad (2)$$

where the operators  $\hat{\Gamma}_{\lambda\mu}^\dagger$  and  $\Gamma_{\lambda\mu}$  create and annihilate the quantum vibrations of the core, characterized by their deformation parameter  $\beta_\lambda$ . In the case of  $1^-$  dipole transitions, we adjust the coupling constants, so that the strength associated with the spurious translational mode is correctly shifted at zero energy. We then treat the interweaving of single-particle motion and of collective degrees of freedom arising within the framework of the Nuclear Field Theory, making use of Bloch-Horowitz perturbation theory [28, 29, 30].

Let us first consider the case of one-neutron halos. The eigenvalues of the dressed single-particle states associated with given angular momenta  $l, j$  ( $s_{1/2}, p_{1/2}$  and  $d_{5/2}$ ) were obtained by diagonalizing energy dependent matrices, schematically shown in the left part of figure 2. The matrix elements connect the basis of unperturbed single-particle states corresponding to the quantum numbers  $n, l, j$ . It is important to notice that once the mean field and the properties of the collective vibrations have been fixed, there are no free parameters in the calculations.

The effect of the renormalization processes on the parity inversion in the case of the valence neutron in  $^{10}\text{Li}$  is shown in the right panel of figure 3. The  $p_{1/2}$  single-particle state is bound by about 1.2 MeV in the initial mean field potential, while there is no  $s_{1/2}$  strength close to threshold. The attractive polarization diagram (figure 2(b), left panel) couples the  $s_{1/2}$  states with intermediate states consisting of one particle plus a vibrational state of the type  $d_{5/2} \otimes 2^+$ , leading to a correlated  $s$  state, lying close to threshold. On the other hand, the repulsive Pauli correction diagram (figure 2(c), left panel), also associated with quadrupole vibrations but involving the  $p_{3/2}$  hole orbital, has a strong effect on the  $p_{1/2}$  state, raising its energy from -1.2 MeV to about +0.5 MeV, and leading to parity inversion. A detailed comparison with experiment in the case of  $^{10}\text{Li}$  requires a consideration of the odd proton, which has been considered as a spectator. A more direct comparison is possible in the case of  $^{11}\text{Be}$ , where one finds  $E_{s_{1/2}} = -0.48$  MeV and  $E_{p_{1/2}} = -0.27$  MeV, to be compared with the experimental values ( $E_{s_{1/2}} = -0.50$  MeV and  $E_{p_{1/2}} = -0.18$  MeV), and with the unperturbed single-particle energies ( $E_{s_{1/2}} \approx 0.14$  MeV and  $E_{p_{1/2}} = -3.12$  MeV). We find a  $d_{5/2}$  state close to threshold. A resonant state is experimentally observed at  $E_{d_{5/2}} = 1.28$  MeV. The  $d_{5/2}$  state lies at higher energy in the case of  $^{10}\text{Li}$ .

We now address the case of the two-neutron halos in  $^{11}\text{Li}$  and  $^{12}\text{Be}$ . The associated energy-dependent matrix is schematically represented in the right part of figure 2. In this case the matrix elements connect pairs of particles lying in the  $s_{1/2}, p_{1/2}$  and  $d_{5/2}$  orbitals coupled to angular momentum and parity  $0^+$ . Although the single-particle states lie in the continuum, coupling states with different number of nodes can lead to a localized wavefunction. We include the matrix elements of the Argonne bare pairing interaction in the  $^1S_0$  channel (indicated by a dashed line in diagram (a)), which can scatter pairs up to high energy. This requires a high value of  $E_{cut}$ ,  $E_{cut} \approx 500$  MeV. We also include the attractive induced interaction arising from the exchange of collective vibrations (see diagram (d)). The exchange of  $1^-$  vibrations is particularly

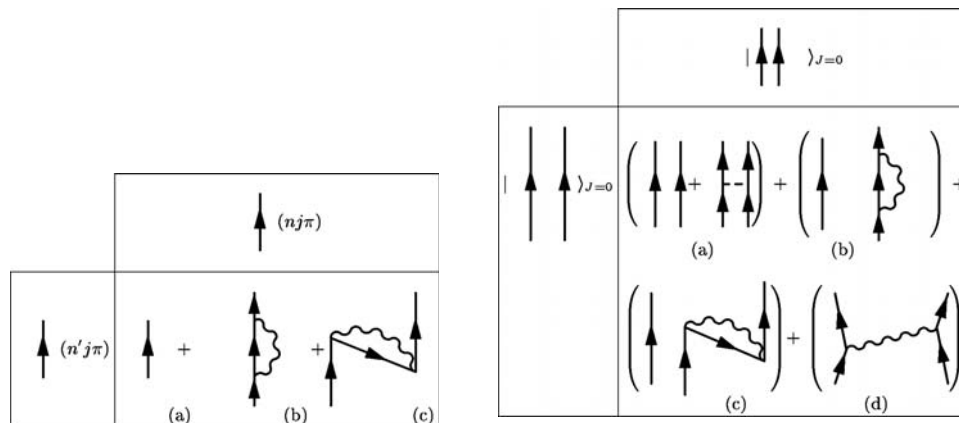


**Figure 2.** Energy-dependent matrices to be diagonalized self-consistently, to obtain the correlated wavefunction for one- (left panel) and two-neutron halo nuclei (right panel) (see Ref. [4]).

important in the case of  $^{11}\text{Li}$ , where substantial dipole strength is found at low energy (pigmy dipole). Most of this low-energy wavefunction is built out of excitations which occupy, to some extent, the same particle states occupied by the loosely bound neutrons we are studying, and the corresponding particle-vibration matrix elements have been corrected from Pauli violating contributions following the nuclear field theory rules (see e.g. [26] and [31]). However, the present RPA calculation of the soft dipole resonance takes explicitly into account its interplay with the giant dipole resonance of the core, and the pigmy dipole wavefunction also includes forwards- and backwardsgoing amplitudes associated with particle-hole transitions involving core orbitals.

The resulting two-neutron separation energies for  $^{11}\text{Li}$  (0.33 MeV) and  $^{12}\text{Be}$  (3.58 MeV) are in overall agreement with the experimental values (0.37 MeV and 3.67 MeV). The effect of the pairing interaction leads from the uncorrelated wavefunction  $|s_{1/2}^2(0)\rangle$  to the correlated one,  $|\tilde{0}\rangle$  (see figure 3 (II) in the case of  $^{11}\text{Li}$ ). The main contribution to the binding energy arises from the induced interaction, while that associated with the bare nucleon-nucleon Argonne potential is quite small (of the order of 100 keV in the case of  $^{11}\text{Li}$ ). The bare interaction is not efficient in coupling low-angular momentum, extended wavefunctions. It is difficult to compare this result with three-body calculations which start from single-particle levels fitted to the experimental value or use density dependent interactions. It is known that the binding energy depends in a delicate way on the assumed position of the resonance energies [21]. We also calculate the energy of the excited  $0^+$  states; in particular, the first excited state in  $^{12}\text{Be}$  is calculated to lie at 2.04 MeV, to be compared with the experimental value of 2.24 MeV.

The diagonalization of the energy-dependent matrix provides detailed information about the "hidden" (virtual) components of the halo wavefunction namely, of the components of the wavefunction involving core vibrations. This, coupled with reaction softwares, leads to definite predictions for the spectroscopic amplitudes and the absolute cross sections associated with one- and two-neutron transfer reactions. We remark that the coupling with core vibrations can affect the radial dependence of transfer form factors in an important way [10, 12, 13, 14, 15], so that a comparison of theory with experiment should be carried out by comparing absolute cross sections. A comparison with spectroscopic factors derived from the experimental cross sections can be at most indicative. With these limitations, the calculated admixture of the  $d_{5/2} \otimes 2^+$  component in the wavefunction of the  $^{11}\text{Be}$  ground state (15%) is to be compared to the value found in the analysis of the  $^{11}\text{Be}(p,d)^{10}\text{Be}$  transfer reaction (17%) [14]. It is also of

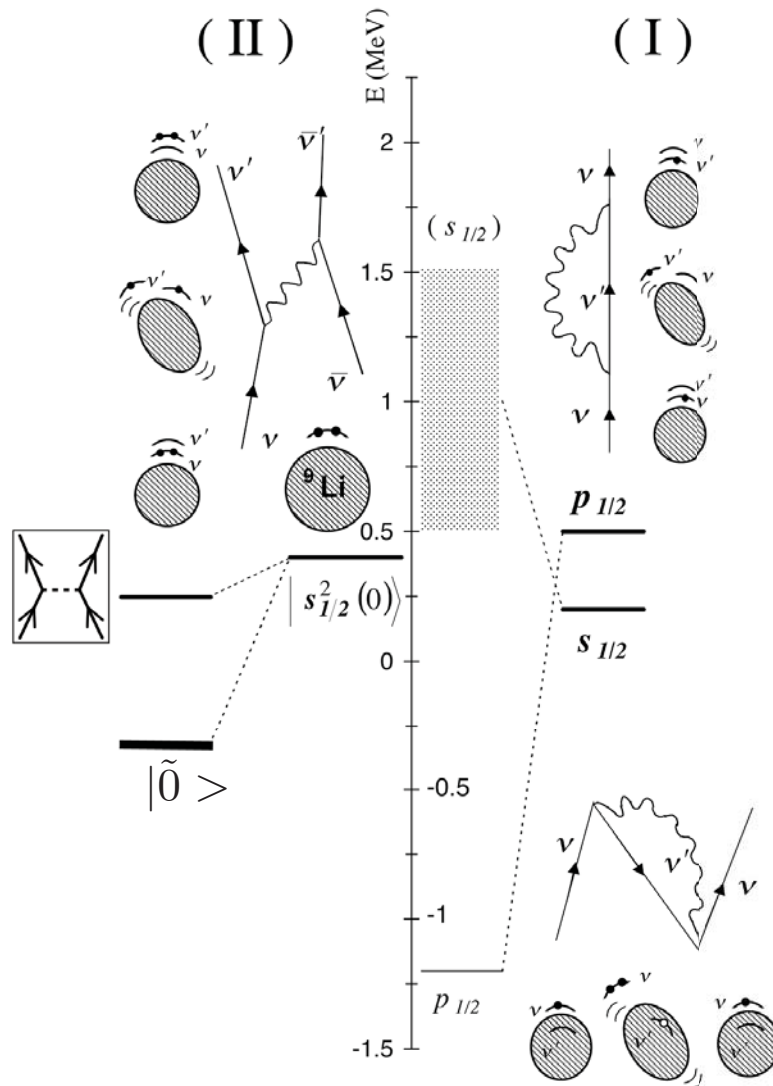


**Figure 3.** Effects of renormalization processes on the halo neutrons in  $^{10}\text{Li}$  (panel I) and in  $^{11}\text{Li}$  (panel II) described in the text (see Ref. [3].)

notice that within the present approach [4] a rather low value ( $S = 0.31$ ) for the spectroscopic factor associated with the  $^{11}\text{Be}(d,p)^{12}\text{Be}(\text{gs})$  reaction was predicted, in agreement with recent experimental findings [32, 33], and at variance with other calculations (see e.g. [34]).

A detailed comparison with experimental absolute cross sections has been carried out for the reaction  $p(^{11}\text{Li}, ^9\text{Li})t$  [35], populating the  $3/2^-$  ground state and the first  $1/2^-$  excited state of  $^9\text{Li}$ . The absolute cross sections for transfer to the  $3/2^-$  ground state and to the  $1/2^-$  first excited state provide a stringent test of the theoretical wavefunction of the  $^{11}\text{Li}$  halo, which can be written as

$$|\tilde{0} \rangle_{\nu} = C|0 \rangle_{\nu} + \alpha|[p_{1/2}, s_{1/2}]_{1^-} \otimes 1^-; 0 \rangle + \beta|[s_{1/2}, d_{5/2}]_{2^+} \otimes 2^+; 0 \rangle, \quad (3)$$

where the calculated coefficients take the value  $C = 0.7$ ,  $\alpha = 0.7$  and  $\beta = 0.1$ , while  $|0 \rangle_{\nu}$  is

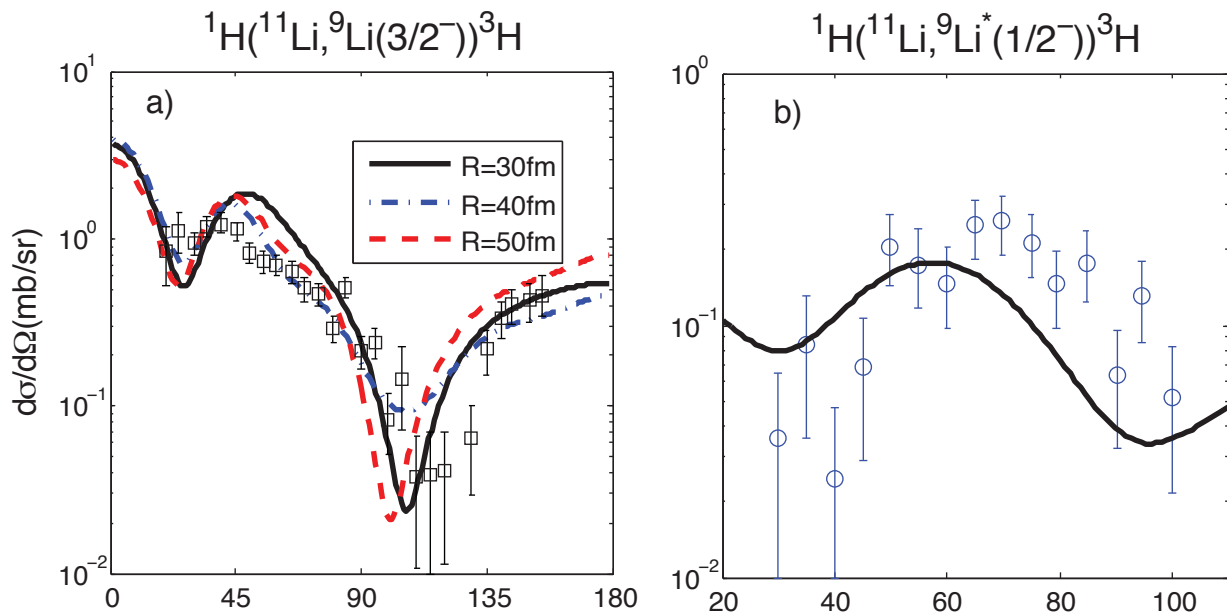


**Figure 4.** (Color online) Theoretical and experimental absolute differential cross sections associated with the  ${}^1\text{H}({}^{11}\text{Li}, {}^9\text{Li}){}^3\text{H}$  two-neutron transfer reaction populating the ground state (a) and the first excited state (b) of  ${}^{11}\text{Li}$ . The three theoretical curves in (a) refer to calculations of the correlated wavefunction  $|0\rangle$  (see equation 3) performed in spherical boxes having different radii  $R$ .

given by

$$|0\rangle_\nu = \sum_{lj, n_1 n_2} a_{n_1 n_2}^{lj} [\psi_{n_1 l j} \psi_{n_2 l j}]_0, \quad (4)$$

where the sum runs over the angular momenta  $(lj) = s_{1/2}, p_{1/2}, d_{5/2}$  and over the number of nodes that identify the different wavefunctions in the discretized continuum. The weight of the different angular momenta is given by

$$\sum_{n_1 n_2} (a_{n_1 n_2}^{lj})^2 = 0.40(s_{1/2}); 0.59(p_{1/2}); 0.003(d_{5/2}). \quad (5)$$

The weight of  $s$  and  $p$  waves is comparable, in overall agreement with the experimental findings. While the ground state transition provides direct evidence on the  $s^2$  and  $p^2$  admixture, which in the present description arises mainly from the phonon induced pairing interaction, it provides no direct evidence for the phonon exchange correlation (note however the normalization  $C^2 = 0.49$  resulting mainly from the coupling to the soft dipole resonance). On the other hand, and in keeping with the fact that the  $1/2^-$  first excited state of  ${}^{11}\text{Li}$  can be viewed as the lowest member of the multiplet obtained by coupling the  $p_{3/2}$  proton to the quadrupole vibration of the core, the associated absolute differential cross section to the  $1/2^-$  state is proportional to the square of the  $\beta^2$  coefficient in equation (3).

The reaction calculation was performed in the second-order DWBA (see [36] and [37] and references therein). Simultaneous, successive and non-orthogonal contributions to the transfer amplitude were taken into account. Global optical potentials were used [35, 38]. The calculation of more reliable optical potentials for the reactions involving halo nuclei, and a better understanding of their connection with elastic scattering represent important open challenges in the field.

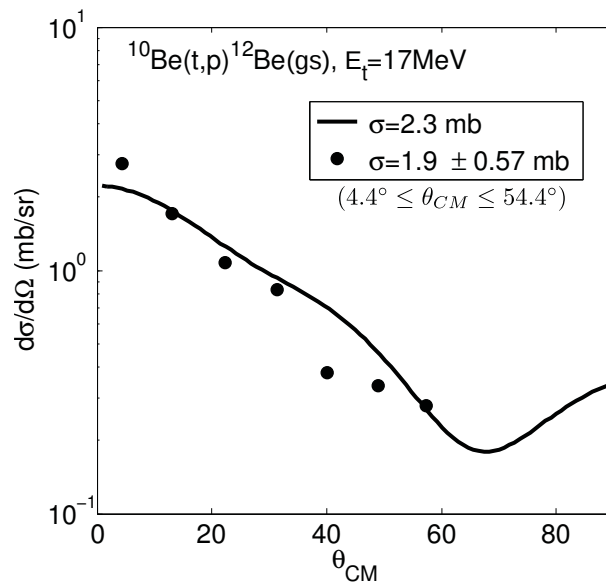


**Figure 5.** Absolute differential cross section measured [40] in the reaction  $^{10}\text{Be}(t,p)^{12}\text{Be}(\text{gs})$  at 17 MeV triton bombarding energy (solid dots). The theoretical calculations (continuous solid curve) were obtained making use of the spectroscopic amplitudes associated with the wavefunction of equation (7), and the optical parameters of Refs. [38] and [40]. The integrated cross sections are shown in the inset (see Ref. [6]).

The calculated cross sections [5] for the transfer to the ground state and to the first excited state of  $^{11}\text{Li}$  are compared to data in figures 4(a) and (b). In (a) we also show that one obtains convergence respect to the box radius  $R$  used in the structure calculation, that is, to calculate the coefficients of the wavefunction (3). It was checked that other channels involving inelastic or breakup processes, which could, in principle, contribute to the transfer to the excited state, turn out to be strongly suppressed as compared to the two-nucleon direct transfer considered here [5, 39].

The wavefunction describing the neutron component of the  $^{12}\text{Be}$  ground state can be written as

$$|\tilde{0}\rangle_{\nu} = C|0\rangle_{\nu} + \alpha|(p_{1/2}, s_{1/2})_{1-} \otimes 1^{-}; 0\rangle + \beta|(s_{1/2}, d_{5/2})_{2+} \otimes 2^{+}; 0\rangle + \gamma|(p_{1/2}, d_{5/2})_{3-} \otimes 3^{-}; 0\rangle, \quad (6)$$

where  $C = 0.87$ ,  $\alpha = 0.10$ ,  $\beta = 0.35$ ,  $\gamma = 0.33$  and (see equations (4) and (5))

$$\sum_{n_1 n_2} (a_{n_1 n_2}^{lj})^2 = 0.19(s_{1/2}); 0.34(p_{1/2}); 0.47(d_{5/2}). \quad (7)$$

The  $d_{5/2}$  orbital plays a much more important role in this case than in  $^{11}\text{Li}$ . The measurement of the reaction  $^{12}\text{Be}(p,t)^{10}\text{Be}$  populating the ground and excited states of  $^{10}\text{Be}$  would provide a stringent test of the wavefunction but it has not yet been made. Within this context, the absolute theoretical [6] and experimental cross sections associated with the reaction  $^{10}\text{Be}(t,p)^{12}\text{Be}$  at 17 MeV triton bombarding energy are compared in figure 5.

The wavefunctions (3) and (6) have been obtained without taking into account the effect of the pairing ground state fluctuations of the core. The latter have been included in calculations of the wavefunction of  $^{12}\text{Be}$  carried out within the particle-particle RPA using both the Gogny [41] and a monopole pairing force [6], and absolute two-neutron transfer cross sections expected within the pair vibrational scheme around  $^{10}\text{Be}$  have also been predicted [6]. In these calculations the

coupling with surface degrees of freedom is not explicitly included, and the positions of the single-particle levels are taken from experiment. A calculation taking into account both pairing and surface ground state fluctuations has not yet been performed.

### 3. Conclusions

Insight in the basic properties of halo nuclei can be obtained taking consistently into account the basic processes associated with vibrations of the system, which renormalize both the single-particle spectrum and the pairing interaction and which can be directly probed with transfer reactions.

### References

- [1] Tanihata I, Savajols H, and Kanungo R 2013 *Prog. Part. Nucl. Phys.* **68** 215
- [2] Broglia R A, Potel G, Barranco F, and Vigezzi E 2010 *J. Phys. G* **37** 064022
- [3] Barranco F, Bortignon P F, Broglia R A, Colò G, and Vigezzi E 2001 *Eur. Jou. Phys. A* **11** 385
- [4] Gori G, Barranco F, Broglia R A, and Vigezzi E 2004 *Phys. Rev. C* **69** 041302(R)
- [5] Potel G, Barranco F, Vigezzi E, and Broglia R A 2010 *Phys. Rev. Lett.* **105** 172502
- [6] Potel G, Idini A, Barranco F, Vigezzi E, and Broglia R A 2012 [ArXiv:1212.2437](https://arxiv.org/abs/1212.2437); *Yad. Fiz.* in press
- [7] Otsuka T, Fukunishi N, and Sagawa H 1993 *Phys. Rev. Lett.* **70** 1385
- [8] Sagawa H, Brown B A, and Esbensen H 1993 *Phys. Lett. B* **309** 1
- [9] Nunes F M, Thompson I J, and Johnson R C 1996 *Nucl. Phys. A* **596** 171
- [10] Nunes F M, Christley J A, Thompson I J, Johnson R C, and Efros V D 1996 *Nucl. Phys. A* **609** 43
- [11] Nunes F M, Thompson I J, and Tostevin J A 2002 *Nucl. Phys. A* **703** 593
- [12] Hamamoto I 1969 *Nucl. Phys. A* **126** 145
- [13] Van de Wiele J, Vdovin A, and Langevin-Joliot H 1996 *Nucl. Phys. A* **605** 173
- [14] Winfield J S *et al.* 2001 *Nucl. Phys. A* **683** 48
- [15] Deltuva A 2013 *Phys. Rev. C* **88** 011601(R)
- [16] Moro A M and Crespo R 2012 *Phys. Rev. C* **85** 054613
- [17] Myo T, Kato K, Toki H, and Ikeda K 2007 *Phys. Rev. C* **76** 024305
- [18] Ikeda K, Myo T, Kato K, and Toki H 2010 *Clusters in nuclei*, Vol 1, Lectures Notes in Physics Vol 818 (Springer)
- [19] Csótó A 1997 [ArXiv:nuc1-th/970454v1](https://arxiv.org/abs/nuc1-th/970454v1)
- [20] Bertsch G F and Esbensen H 1991 *Ann. Phys.* **209** 327
- [21] Zhukov M V, Danilin B V, and Fedorov D V 1993 *Phys. Rep.* **231** 151
- [22] Hagino K, Sagawa H, Carbonell J, and Schuck P 2007 *Phys. Rev. Lett.* **99** 022506
- [23] Forssen C, Caurier E, and Navratil P 2009 *Phys. Rev. C* **79** 021303(R)
- [24] Nörterhäuser W, Neff T, Sánchez R, and Sick I 2011 *Phys. Rev. C* **84** 024307
- [25] Liu L, Otsuka T, Shimizu N, Utsuno Y, and Roth R 2012 *Phys. Rev. C* **86** 014302
- [26] Bohr A and Mottelson B R 1975 *Nuclear Structure*, Vol. II (Benjamin)
- [27] Bohr A and Mottelson B R 1969 *Nuclear Structure*, Vol. I (Benjamin)
- [28] Bès D R, Broglia R A, Dussel G G, Liotta R J, and Sofía H M 1976 *Nucl. Phys. A* **260** 1
- [29] Bès D R, Broglia R A, Dussel G G, Liotta R J, and Sofía H M 1976 *Nucl. Phys. A* **260** 27
- [30] Bès D R, Broglia R A, Dussel G G, Liotta R J, and Perazzo R J 1976 *Nucl. Phys. A* **260** 77
- [31] Bortignon P F, Broglia R A, Bes D R, and Liotta R J 1977 *Phys. Rep.* **30** 305
- [32] Kanungo R *et al.* 2010 *Phys. Lett. B* **682** 391
- [33] Johansen J G *et al.* 2013 *Phys. Rev. C* **88** 044619
- [34] Fortune H T and Sherr R 2012 *Phys. Rev. C* **85** 051303(R)
- [35] Tanihata I *et al.* 2008 *Phys. Rev. Lett.* **100** 192502
- [36] Bayman B F and Chen J 1982 *Phys. Rev. C* **26** 1509
- [37] Potel G, Idini A, Barranco F, Vigezzi E, and Broglia R A 2013 *Rep. Prog. Phys.* **76** 106301
- [38] An H and Cai C 2006 *Phys. Rev. C* **73** 054605
- [39] Vigezzi E, Potel G, Barranco F, and Broglia R A 2011 *J. Phys. G. Conf. Ser.* **312** 092061
- [40] Fortune H T, Liu G B, and Alburger D E 1994 *Phys. Rev. C* **50** 1355
- [41] Blanchon G, Vinh Mau N, Bonaccorso A, Dupuis M, and Pillet N 2010 *Phys. Rev. C* **82** 034313